EFFECTS OF GROUND WATER TABLE AND GROUND INCLINATION ON TRAIN INDUCED GROUND-BORNE VIBRATIONS

C. BAYINDIR[1], §

ABSTRACT. Passage of the train wheels induces ground-borne vibrations at the rail-wheel interface, where the main contribution is due to the axle loads moving on irregular track and wheel interface. These vibrations can cause problems such as the compaction and settlement of the foundation soil of the structures nearby, liquefaction of the soil or discomfort of people, just to name a few. Therefore predicting and controlling such phenomena is critically important for the design and operation of the railways. These vibrations are modeled using many different methods existing in the literature. In this paper we analyze the effects of groundwater depth and ground inclination angle on those vibrations using a random vibration model, where the elastic rail-soil system is modeled as a Winkler foundation. We examine the effects of changing fully saturated groundwater levels and changing ground inclination angles on such vibrations. We relate the groundwater depth and ground inclination angle parameters with the stiffness of the Winkler model using Terzaghi's, Vesic's and Bowles's bearing capacity formulas. The common 5-axle and the 6-axle tram load configurations and different train speeds of 30 km/hr, 40 km/hr, 50 km/hr are used in our implemented model. It is shown that the decrease in groundwater depth and/or higher ground inclination angle can significantly change the peak and rms vibration velocity and acceleration levels, both for the 5-axle and 6-axle configurations and all three different train speeds. We present exponential and exponential-trigonometric fit curves to the results of the implemented random vibration model, which can be used to model the approximate changes in the ground-borne vibration velocity and acceleration levels due to different groundwater depth and different ground inclination angles. We also discuss our results and their applicability.

Keywords: Train induced vibrations, Winkler foundation, Random vibrations, Groundwater table, Ground inclination angle.

AMS Subject Classification: 74H50, 74H10, 35Q74

1. INTRODUCTION

Ground-borne vibrations induced by the moving railway trains can cause many problems including but are not limited to compaction of the foundation soil of the structures nearby, excessive settlement and differential settlement, soil liquefaction and structural vibrations that may discomfort people in the frequency interval of $1 - 80 \ Hz$ [1, 2, 3]. Therefore

[1] Associate Professor, Engineering Faculty, İstanbul Technical University, 34467, Maslak, İstanbul.
  Adjunct Professor, Engineering Faculty, Boğaziçi University, 34342, Bebek, İstanbul.
  e-mail: cihan.bayindir@isikun.edu.tr; ORCID: http://orcid.org/0000-0002-3654-0469.

it is crucially important to model, measure and analyze those vibrations, especially when high risk buildings are located in the vicinity of the railways. Many different analytical, numerical and/or experimental techniques are proposed and used in the literature in order to model such vibrations, such as [1, 2, 3, 4, 5, 6, 7, 8, 9, 10, 11]. In analytical techniques, the elastic foundation beneath the railway track is commonly modeled in the frame of the elastic beam theories, such as the Euler-Bernoulli or the Timoshenko beam [1, 2, 3, 4, 5, 6, 7] and different loading scenarios such as harmonic loading or point loading due to moving axles are considered [4, 5]. When the effect of vertical soil stiffness is included, the rail on the surface of the soil can be modeled using the commonly used Euler-Bernoulli beam placed on elastic foundation analogy, which is also known as Winkler foundation model [1, 2]. Generally, the formulation and solution of this Winkler problem is performed in spectral domain since convolutions are costly to compute and vibrations standards such as ISO 2631, DIN 4250-3 are given in spectral domain. In empirical methods, measurements of the ground vibration from railway trains are validated with the results of models [8]. The most common numerical method used to model the railway behavior is the finite element method, which can be used to analyze general 3D structures resting on an elastic half-space under rail [1]. There are some other studies which utilizes the coupled finite element-boundary element methods to model railway induced vibrations [1]. We refer the reader to [1] for a more comprehensive discussion of the existing literature.

Although ground-borne vibrations generated at the railway on rail wheel interface are well studied using different models mentioned above, there are only very few studies existing in the literature which analyzes them when the soil and subgrade are stiffened [24, 25]. There are even fewer studies analyzing the effects of loosening of the subsoil on ground-borne train vibrations. One of the papers existing in the literature is analyzing the effects of the ground water table on traffic induced vibrations [26]. In that paper, authors investigate the influence of the depth of the ground water table in a dry homogeneous reference half-space on traffic induced vibrations, where they model the soil as a single layer on a half-space which represents the saturated soil [26]. Their study showed that the presence of the ground water decreases the compressibility of the soil due to the presence of the pore fluid, resonance of the dry layer may occur and additionally refracted P-waves in the dry layer interfere with surface waves [26]. Another study had addressed the effects of inclined soil layers on surface vibrations from underground railways [27], where authors have used a semi-analytical approach called thin layer method. They have investigated the effects of the ground inclinations up to 5° on the surface ground-borne vibrations generated by underground railways and showed that significant variation in RMS response of approximately 5 dB may happen [27]. Since, to our best knowledge, there is no research examining the direct effects of decrease in the soil stiffness of the subgrade soil on ground-borne vibrations induced by moving trains on the ground, we aim to address this open problem. With this motivation we analyze the effects of changing ground water depth and various ground inclination angles on railway induced ground-borne vibrations, considering the railways constructed near a slope or cliff. The use simple and easily implementable Winkler foundation model and use Terzaghi's, Vesic's and Bowles's bearing capacity and stiffness relations to relate the stiffness of the Winkler foundation with ground water depth and the ground inclination angle (or slope), assuming that linear elastic problem remains linear elastic under these circumstances. Utilizing a random vibration model for train induced ground-borne vibrations, we investigate the changes in the levels of vibration parameters due to changing groundwater depth and ground inclination angles, where we also provide approximate relations.

2. Methodology

In order to discuss the effects of the depth of the groundwater table and the ground inclination on the railway induced ground-borne vibrations, we implement a random vibration model which was introduced in [1, 2]. The model is a random vibration model of a simple slab beam which rests on elastic foundation. Therefore railway beam and foundation beneath is modeled as a Winkler foundation. The transfer functions are used to relate the displacement of the Winkler foundation to the ground-borne vibration velocities and accelerations, where the spectral approach is utilized to take the roughness spectrum into account. Then rms vibration velocities and accelerations are derived from the spectral density of the vibrations and accelerations. The reader is referred to [1, 2] for a more comprehensive discussion of this model.

2.1. **Review of the Random Vibration Model for a Simple Slab Beam.** Displacement of a simple slab beam, $y(x)$, can be computed by the convolution in x domain, that is using

$$y(x) = \int_{-\infty}^{\infty} H(x - \chi)Q(\chi)d\chi \tag{1}$$

where $Q(\chi)$ is the force per unit length acting along the rail [1, 2]. In here, $H(x)$ is the frequency response function for the displacement, $y(x)$, at the loading point which is $x = 0$ [1, 2]. Since the convolution operations are computationally costly and critical threshold levels specified in some standards such as ISO 2631, DIN 4250-3 are spectral, we formulate this problem spectrally, that is using Fourier analysis. Some applications, uses and advantages of the Fourier and beyond spectral analysis can be seen in [12, 13, 14, 15, 16, 17, 18, 19, 20, 21, 22, 23]. If we take the Fourier transform of Eq.1, we obtain

$$\tilde{Y}(\xi) = \tilde{H}(\xi)\tilde{Q}(\xi) \tag{2}$$

In here, $\tilde{H}(\xi)$ is the frequency response function in the wavenumber domain. If the displacements are small, then dynamics of the slab beam can be modeled using linear Euler-Bernoulli beam formula. Adding the vertical force due to compression of the soil analogously to the spring force, the governing equations becomes the Winkler model for elastic foundation. Winkler foundation can be modeled using

$$m\frac{\partial^2 y(x,t)}{\partial t^2} + EI\frac{\partial^4 y(x,t)}{\partial x^4} + k_w y(x,t) = f(x,t) \tag{3}$$

where k_w is the soil stiffness. Analogous to serially connected springs, the stiffness of the Winkler foundation can be formulated using

$$\frac{1}{k_w} = \frac{1}{k_{sb}} + \frac{1}{k_r} \tag{4}$$

where k_r and k_{sb} are the stiffnesses of the rail pad and subsoil-ballast, respectively. The railpad stiffness is taken as $k_r = 30 \times 10^6 N/m/m$ in our calculations which represents a typical value. The soil-ballast stiffness, k_{sb}, is measured at different points in construction site using geotechnical instrumentation. A critically low value of $4125kN/m/m$ is measured at an ongoing construction site in Eyüp, İstanbul where many historical buildings which some are built by Archtitect Sinan [28]. This value is used throughout this paper. In order take the dissipative effects of the rail pad and subsoil into account, a constant loss factor of $\eta = 0.09$ is used [1, 2]. Therefore, k_w is multiplied with a factor of $(1 + i\eta)$ [1, 2]. The Winkler frequency response $Y(x, \omega)$ is obtained by appyling Eq.3 to an infinite

beam on an elastic foundation [1, 2]. This leads to

$$Y(x,\omega) = \frac{1}{4\alpha^3 EI}(e^{\alpha|x|} + ie^{i\alpha|x|}) \tag{5}$$

where

$$\alpha^4 = \frac{m\omega^2 - k_w}{EI} \tag{6}$$

The root *alpha* given in Eq.5 is selected to be in the second quadrant to guarantee that both exponentials decay as $|x| \to \infty$ [1, 2]. Therefore the Winkler frequency response, $Y(x,\omega)$, at $x = 0$ becomes

$$\tilde{Y}(x=0,\omega) = \frac{1}{4\alpha^3 EI}(1+i) = \tilde{H}(\omega) \tag{7}$$

We assume that all train wheels are smooth and the irregularities are only in the rail surface. The axle load inputs can differ by a time delay [1, 2]. The time delay between two axles of indices p and q, is $T = L_{pq}/v$. Here, L_{pq} shows the nonuniform axle spacing between these two axles and v shows the speed of the train. Three different train speeds of 30 km/hr, 40 km/hr and 50 km/hr are considered in this study. With these assumptions and using random vibration theory, the output spectrum of the vertical rail displacement can be computed using [21]

$$S(\omega) = \sum_{p=1}^{N}\sum_{q=1}^{N} H_p^*(\omega)H_q(\omega)S_o(\omega)e^{-i\omega L_{pq}/v} \tag{8}$$

where p and q are axle indices. Here, $H_p(\omega)$ and $H_q(\omega)$ denotes the frequency response functions of axle p and q loadings, respectively which are calculated using Eq.7. Since the designed railway will be used for operations of trams, two common tram configurations with 5 and 6 axle spacings are considered in this study. The L_{pq} distances are computed using these configurations which are shown in Fig.1. Trams modeled in this study is considered to have two wagons and 1m buffer between two wagons, both for the 5-axle and 6-axle configurations is used. In Eq.8, $S_o(\omega)$ shows the two sided rail roughness spectrum. This two sided spectrum can be calculated using the one-sided rail roughness spectrum by $S_o(f) = 4\pi S_o(\omega)$ where $\omega = 2\pi f$. One of the most common forms of rail roughness spectrum is given in [29] and given as

$$S_o(f) = \frac{1}{v}\frac{a}{(b+f/v)^3} \tag{9}$$

The parameters of a and b of this formulation are tabulated in Table 1 for different rail conditions.

TABLE 1. Rail roughness parameters for different rail conditions.

Rail Condition	$a(mm^2.(1/m)^2)$	$b(1/m)$
Worst	9.39×10^{-1}	6.89×10^{-2}
Average	1.31×10^{-2}	2.94×10^{-2}
Best	1.90×10^{-4}	9.71×10^{-3}

Throughout this paper, the worst rail conditions are considered and parameters a and b are selected accordingly. Once the output displacement spectrum, $S_y(\omega)$, is obtained, the mean square value of the vertical rail displacement can be computed by

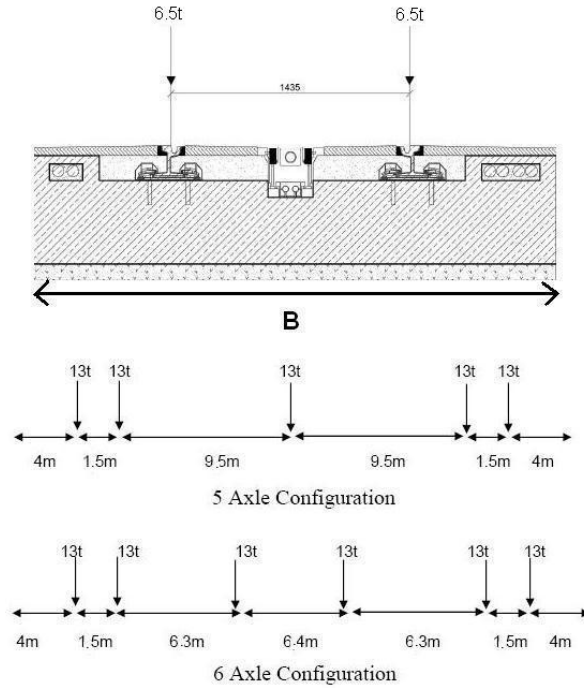$$E[y^2] = \int_{-\infty}^{\infty} S_y(\omega)d\omega \tag{10}$$

FIGURE 1. a) Railway track foundation b) 5 axle and 6 axle train load configurations used in the calculations.

By taking the square root of this expression one can eventually obtain the rms vertical displacement values, y_{rms}. Similary, using the theory of random vibrations [21], the output spectrum for vertical vibration velocity and acceleration becomes

$$S_v(\omega) = \omega^2 S_y(\omega) \tag{11}$$

and

$$S_a(\omega) = \omega^2 S_v(\omega) = \omega^4 S_y(\omega) \tag{12}$$

Finally, the rms values of the vibration velocity and acceleration, v_{rms} and a_{rms}, can be calculated using

$$E[v^2] = \int_{-\infty}^{\infty} S_v(\omega) d\omega \tag{13}$$

and

$$E[a^2] = \int_{-\infty}^{\infty} S_a(\omega) d\omega \tag{14}$$

Generally, for the assessment of the results and checking the threshold criteria, the frequency axis is divided into 1/3 octave bands and averaging is performed within each 1/3 octave band. For illustrative purposes, a representative velocity spectral density obtained using the method summarized above is depicted Fig.2 for 5-axle configuration, which is reaching a peak V_{rms} value of 3.21 mm/s for V=40km/hr train speed. Additionally, a typical acceleration spectral density obtained using the method summarized above is depicted Fig.3 for 6-axle configuration, which is reaching a peak a_{rms} value of 0.22 mm/s^2 for V=40km/hr train speed. While these results represent the conditions for deep ground water table and horizontal ground inclination, we extend this random vibration model
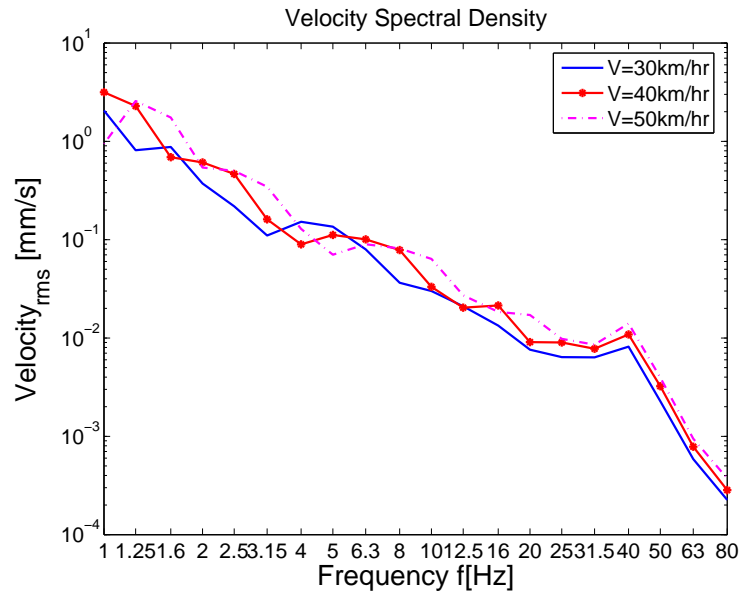
FIGURE 2. A representative spectral density of the ground-borne vibration velocity obtained using 5-axle train configuration.
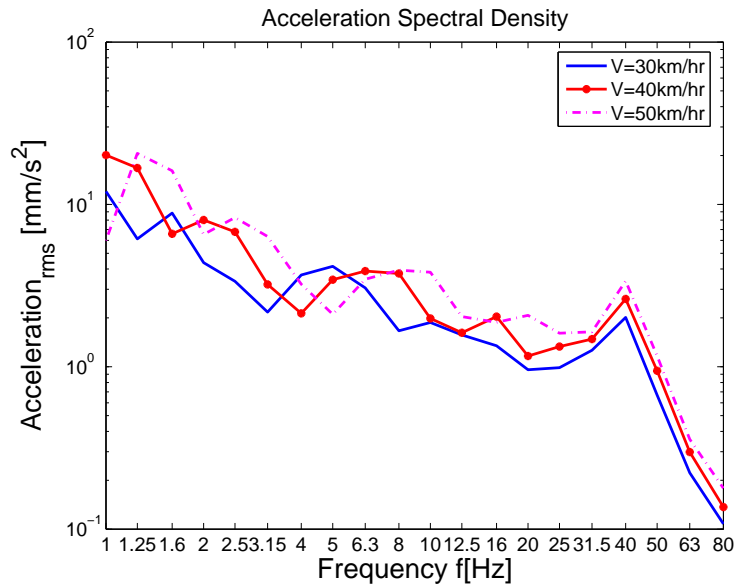

FIGURE 3. A representative spectral density of the ground-borne vibration acceleration obtained using 6-axle train configuration.

to account for different ground water levels and different ground inclinations in the next section.

2.2. **Modeling the effects of ground water level and the ground inclination angle on the ground-borne vibrations.** High railway-induced ground vibration levels are often associated with poor ground conditions of the railway track's subsoil [1, 2, 3, 7]. Therefore stiffening of the subgrade under the railway track is generally considered as the

first possible solution to reduce the ground-borne vibration levels. Few studies do exist for this purpose, such as those discussing the effects of soil improvement due to subgrade stiffening and stiff inclusions [25]. However decrease of the stiffness of the subsoil due to increasing ground water table and/or higher ground inclination angles are not accounted for in these studies. In this paper, we attempt to attack this problem and discuss the effects of change in ground water level and different ground inclination angles on the ground-borne vibration levels using the random vibration model summarized above. Well known Bowles's formula can be used to relate the soil-ballast stiffness, k_{sb}, with its bearing capacity, q. This formula reads [30]

$$k_{sb} = 40 \times SF \times q \qquad (15)$$

Here, SF is an empirical constant. Although this equation provides an empirical relation, it is easy to check that k_{sb} is linearly proportional to q in theory, as well. In order to take the effects of changing fully saturated ground water levels and different ground inclinations into account, we turn our attention to Terzaghi's bearing capacity formula

$$q_{ult} = c'N_c + \sigma'_{zD}N_q + 0.5\gamma'BN_\gamma \qquad (16)$$

where q_{ult} is the ultimate bearing capacity, c' is the effective cohesion beneath the foundation, σ'_{zD} is the effective stress at depth D which is the depth of foundation, γ' is the effective unit weight of soil, B is the width of foundation and N_c, N_q, N_γ are the Terzaghi's bearing capacity factors which are functions of the effective internal friction angle, ϕ', [31]. This formula is extended by Vesic to take the effects of various foundation shapes, depths, load inclinations, base inclinations and ground inclinations into account and their applicability conditions are discussed in [31]. In this study, we restrict ourselves to cohensionless soils, that is $c' = 0$. Additionally, since the proposed tramway line rests on the ground level, its foundation depth can be taken as $D \approx 0$. Therefore, under these approximations Eq. 16 becomes

$$q_{ult} = 0.5\gamma'BN_\gamma \qquad (17)$$

Considering railway design practice, base and load inclinations are not very common. Depending on the location of the track, the ground inclination can be important. Under these approximations, the bearing capacity formula extended by Vesic reads as

$$q_{ult} = 0.5\gamma'BN_\gamma g_\gamma \qquad (18)$$

where

$$g_\gamma = [1 - \tan(\beta)]^2 \qquad (19)$$

is the ground inclination factor. Here, β is the ground inclination angle defined from the horizontal in degrees as discussed in Coduto (see Ch. 6) [31]. Depending on the depth of the water table, the effective unit weight in Eq. 17 can be taken as

- Case 1: if $D_w \leq D$ then $\gamma' = \gamma_b = \gamma - \gamma_w$
- Case 2: if $D < D_w < D + B$ then $\gamma' = \gamma - \gamma_w \left(1 - (D_w - D)/B\right)$
- Case 3: if $D + B \leq D_w$ then $\gamma' = \gamma$

where D_w is the depth of the groundwater table, B is the width of the foundation which is taken as 2m and D is the depth of the foundation, which is taken as 0m in this study. Therefore the relative groundwater depth, D_w/B, and the ground inclination angle (banking angle), β, can be directly related to the stiffness of the Winkler foundation using Case2 and Eqs. 15, 16 and 18.

3. Results and Discussion

The increase of the normalized vibration velocity as a function of increasing relative groundwater depth, D_w/B, is depicted in Fig.4 both for the 5-axle and 6-axle configurations. Normalization value is selected either by choosing the peak or rms vibration velocity for all three train speeds when groundwater is deep enough to be classified as Case 3. Then by changing the relative groundwater depth parameter, D_w/B, the ground-borne vibration velocities for three different train speeds are obtained and normalized by the normalization value. All three train speeds of 30 km/hr, 40 km/hr and 50 km/hr result in the same curve, both for the 5-axle and 6-axle loading conditions. It is useful to note that Fig.4 has two x axes, where the second x axis shows the k_{sb} values corresponding to different D_w/B values.
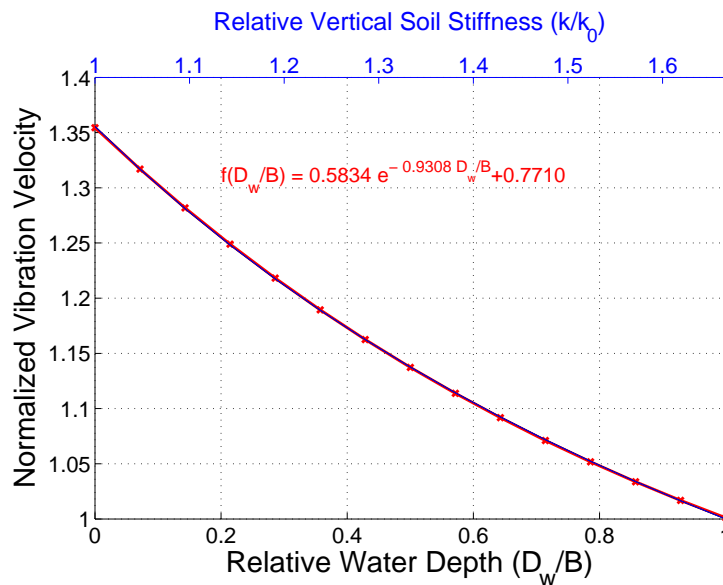

FIGURE 4. Normalized ground-borne vibration velocity as a function of the relative groundwater depth, D_w/B.

Checking Fig.4, one can realize that when ground water table comes to the same level with ground surface, that is when $D_w/B = 0$, ground-borne vibration velocity increases to a level of approximately 1.36 times its maximum value (approximately 2.7 dB increase in amplitude) at dry soil conditions. In this formulation we assume that the change in the groundwater table does only effect the stiffness of the subsoil in our model and linear elastic Winkler foundation remains linear elastic.

Fitting an exponential to the curve obtained by the implemented model in Fig.4 in the least squares sense, we come up with an equation in the form of

$$V_{gwt}(D_w/B) \approx V \times f(D_w/B) \approx V \times (0.5834e^{-0.9308 \times D_w/B} + 0.7710) \qquad (20)$$

In here V can be the peak or rms ground-borne vertical vibration velocity when $D_w/B = 0$. V_{gwt} shows the corresponding peak or rms vertical ground-borne vibration velocity as a function of relative groundwater depth. Therefore under the assumptions and approximations made, this equation can be used to estimate the ground-borne vibration velocities for different D_w/B, once the actual ground-borne vibration velocities are known for dry or wet soil conditions. Checking Fig.5, we can see that same curve and same conclusions
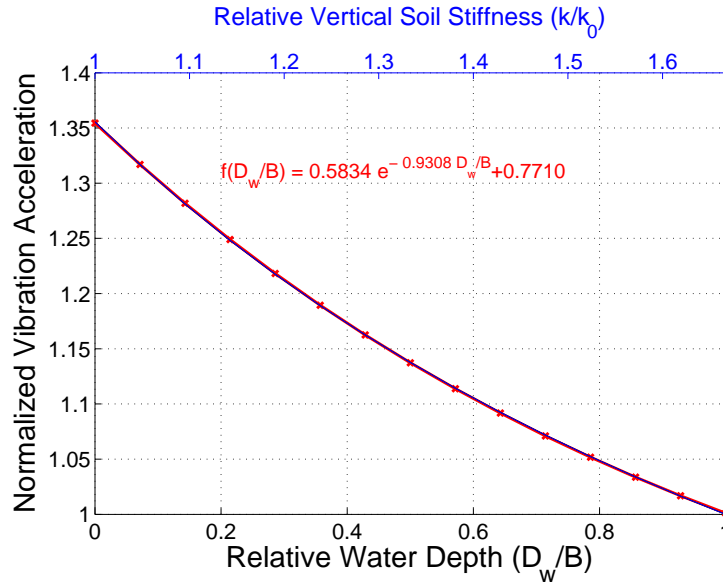
FIGURE 5. Normalized ground-borne vibration acceleration as a function of the relative groundwater depth, D_w/B.

are also valid for ground-borne acceleration levels, for all three train speeds considered. Therefore, similarly, once the actual ground-borne acceleration level are known for either dry or wet soil conditions, the acceleration values for different D_w/B can be estimated using

$$a_{gwt}(D_w/B) \approx a \times f(D_w/B) \approx a \times (0.5834e^{-0.9308 \times D_w/B} + 0.7710) \qquad (21)$$

where a can be the peak or rms vertical ground-borne vibration acceleration when $D_w/B = 0$. Thus a_{gwt} is the corresponding peak or rms vertical ground-borne vibration acceleration which is a function of D_w/B.

The increase of the normalized ground-borne vibration acceleration as a function of increasing ground inclination (banking) angle , β, is depicted in Fig.6. As before, both the 5-axle and 6-axle configurations lead to similar results. Normalization of the acceleration values is performed in a manner similar to the normalizations of the velocities, however in this process for all three different train speeds the peak or the rms acceleration is selected as a normalization factor obtained for ground inclination angle of $\beta = 0$, that is for the horizontal ground. Again, Fig.6 has two x axes, where the second x axis shows the k_{sb} values corresponding to different β values calculated using Vesic's and Bowles's formulas. Depending on the ground inclination angle β, ground-borne vibration velocity and accelerations increases to a level of approximately 5.70 times of their maximum (approximately 15.2 dB increase in amplitude) for the horizontal ground conditions.

Approximating the curve obtained using the model by an exponential-trigonometric fit in the least squares sense, one can come up with an equation in the form of

$$V_{\beta}(\beta) \approx V \times f(\beta) \approx V \times (0.1074e^{5.1917 \tan(\beta)} + 0.9754) \qquad (22)$$

where β is in degrees. Again, in here V denotes the peak or the rms vertical vibration velocity when ground is level, that is $\beta = 0$. Thus V_{β} becomes the corresponding peak or rms vertical vibration velocity as a function of changing ground inclination angle, β.

Checking Fig.7, it is possible to state that conclusions drawn for ground-borne vibration velocities are only slightly different than those of ground-borne accelerations, for all three
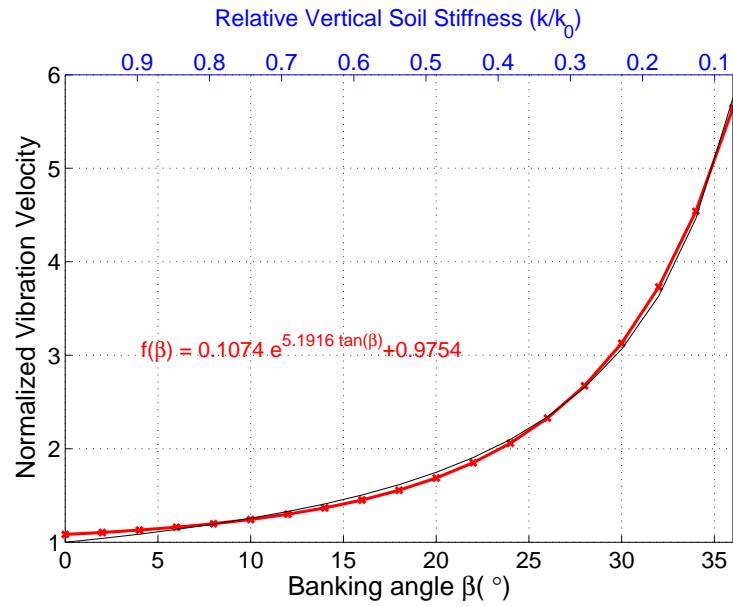
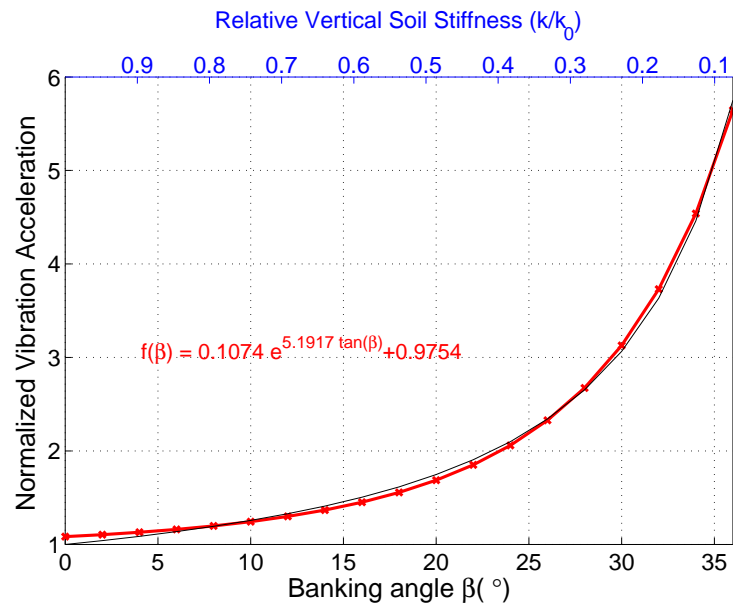FIGURE 6. Normalized ground-borne vibration velocity as a function of ground inclination angle, β.

FIGURE 7. Normalized ground-borne vibration acceleration as a function of ground inclination angle, β.

different train speeds modeled. Therefore, once the actual ground-borne acceleration levels are known for any ground inclination angle β, the acceleration values for different β values can safely be estimated using

$$a_\beta(\beta) \approx a \times f(\beta) \approx a \times (0.1074e^{5.1917\tan(\beta)} + 0.9754) \tag{23}$$

Similarly, in here a shows the peak or the rms vertical ground-borne vibration acceleration for horizontal ground, $\beta = 0$. Thus a_β becomes the corresponding peak or rms vertical vibration acceleration as a function of ground inclination angle, β.

It is useful to note that when not only the groundwater level is close to ground surface and but also when the railway track is constructed in the vicinity of a ground slope, subsoil stiffness can be adjusted to include this combined effect using the Terzaghi's, Vesic's and Bowles's formulas and the random vibration model can be implemented for that stiffness to determine expected ground-borne vibration levels. Additionally, other stiffness effecting factors, such as the load or shape inclinations, surcharge terms, cohension properties of the soils, using geosynthetics beneath the track just to name a few, can be modeled using the approach presented in this paper.

4. Conclusion and Future Work

In this paper we have examined the effects of groundwater depth and ground inclination angle on the ground-borne vibration levels induced by moving trains. More specifically, we have implemented a random vibration model of a Winkler foundation which can be considered as a model of elastic rail resting on elastic soil. The decrease in the vertical stiffness of the foundation soil was directly related with the ground water depth and ground inclination angle using the Terzaghi's, Vesic's and Bowles's bearing capacity formulas. The 5-axle and the 6-axle train configurations, which are commonly used in tramway industry worldwide, are considered and the model was implemented for different train velocities of 30 km/hr, 40 km/hr, 50 km/hr. Typical railway design parameters are selected and the soil parameters measured at a tramway line construction site in İstanbul is used in the Winkler foundation model. In our study, it is shown that the change in the vertical stiffness of the foundation due to changing groundwater depth and/or changing ground inclination angle can significantly change the peak and rms vibration levels both for the 5-axle and 6-axle configurations. Our results indicate that the all three train velocities of 30 km/hr, 40 km/hr and 50 km/hr lead to similar results, both for the 5-axle and 6-axle configurations. Our results also indicate that the effect of ground inclination angle would be more significant in this respect. Additionally, we have provided approximate exponential and exponential-trigonometric fit curves as functions of relative groundwater depth, D_w/B, and the ground inclination angle, β, which can be used to estimate the increased ground-borne vibration velocity and acceleration levels (peak or rms) due to changing groundwater depth and/or ground inclination angles.

References

[1] Forrest, J. A. and Hunt, H. E. M., (2006), A three-dimensional tunnel model for calculation of train-induced ground vibration, Journal of Sound and Vibration, 294, 4, pp. 678-705.

[2] Forrest, J. A. and Hunt, H. E. M., (2006), Ground vibration generated by trains in underground tunnels, Journal of Sound and Vibration, 294, 4, pp. 706-736.

[3] Bayındır, C., Kesten, A. S. and Etminan, E., (2018), A Theoretical Method for the Investigation of the Effects of Soil Improvement on Train Induced Ground-Borne Vibrations, 13th International Conference on Advances in Civil Engineering, Izmir, Turkey.

[4] Sheng, X., Jones, C. J. C. and Petyt, M., (1999), Ground vibration generated by a harmonic load acting on a railway track, Journal of Sound and Vibration, 225, 1, pp. 3-28.

[5] Sheng, X., Jones, C. J. C. and Petyt, M., (1999), Ground vibration generated by a load moving along a railway track, Journal of Sound and Vibration, 228, 1, pp. 129-156.

[6] Jones, C. J. C., Sheng, X. and Petyt, M., (2000), Simulations of ground vibration from a moving harmonic load on a railway track, Journal of Sound and Vibration, 231, 3, pp. 739-751.

[7] Bayındır, C., (2018), Efficient Sensing of Ground-Borne Vibrations Induced by Pile Driving using Compressive Sampling, Researchgate Preprint 10.13140/RG.2.2.16837.09444.

[8] Persson, N., (2016), Predicting Railway-Induced Ground Vibrations, M.S. Thesis, Lund University.

[9] Sheng, X., Jones, C. J. C. and Thompson, D. J., (2003), A comparison of a theoretical model for quasi-statically and dynamically induced environmental vibration from trains with measurements, Journal of Sound and Vibration, 267, 3, pp. 621-635.

[10] Sheng, X., Jones, C. J. C. and Thompson, D. J., (2004), A theoretical study on the influence of the track on train-induced ground vibration, Journal of Sound and Vibration, 272, 3, pp. 909-936.

[11] Sheng, X., Jones, C. J. C. and Thompson, D. J., (2004), A theoretical model for ground vibration from trains generated by vertical track irregularities, Journal of Sound and Vibration, 272, 3, pp. 937-965.

[12] Bayındır, C., (2009), Implementation of a Computational Model for Random Directional Seas and Underwater Acoustics, M.S. Thesis. University of Delaware.

[13] Canuto, C., (2006), Spectral Methods: Fundamentals in Single Domains. Springer-Verlag, Berlin.

[14] Demiray, H. and Bayındır, C., (2015), A note on the cylindrical solitary waves in an electron-acoustic plasma with vortex electron distribution, Physics of Plasmas, 22, 092105.

[15] Karjadi, E. A., Badiey, M., Kirby, J. T. and Bayındır, C., (2012), The effects of surface gravity waves on high-frequency acoustic propagation in shallow water, IEEE Journal of Oceanic Engineering, 37, pp. 112-121.

[16] Bayındır, C., (2015), Compressive split step Fourier method, Journal of Applied and Engineering Mathematics, 5, 2, pp. 298-306.

[17] Bayındır, C., (2016), Compressive spectral method for the simulation of the nonlinear gravity waves, Scientific Reports, 22100.

[18] Bayındır, C., (2016), Rogue waves of the Kundu-Eckhaus equation in a chaotic wave field, Physical Review E, 93, 032201.

[19] Santamarina, J. C., Klein, K. A. and Fam, M. A., (2001), Soils and Waves: Particulate Materials Behavior, Wiley.

[20] Bayındır, C., (2016), Rogue wave spectra of the Kundu-Eckhaus equation, Physical Review E, 93, 062215.

[21] Newland, D. E., (1993), An Introduction to Random Vibrations, Spectral & Wavelet Analysis. Longman, London.

[22] Trefethen, L. N., (2000), Spectral Methods in MATLAB. SIAM, Philadelphia.

[23] Bayındır, C., (2016), Early detection of rogue waves by the wavelet transforms, Physics Letters A, 380, 1, pp. 156-161.

[24] Jiang, J., Toward, M. G. R., Dijckmans, A. and Thompson, D. J., (2014), The influence of soil conditions on railway induced ground-borne vibration and relevant mitigation measures, The 21st International Congress on Sound and Vibration, pp. 2895-2904.

[25] Thompson, D. J., Jiang, J., Toward, M. G. R., Hussein, M. F. M., Dijckmans, A., Coulier, P., Degrande, G. and Loambert, G., (2015), The mitigation of railway-induced vibration by using subgrade stiffening, Soil Dynamics and Earthquake Engineering, 79, pp. 89-103.

[26] Schevenels, M., Degrande, G. and Lombaert, G., (2004), The influence of the depth of the ground water table on free field road traffic-induced vibrations, International Journal for Numerical and Analytical Methods in Geomechanics, 28, pp. 395-419.

[27] Jones, S. and Hunt, H., (2011), Effect of inclined soil layers on surface vibration from underground railways using the thin-layer method, Journal of engineering mechanics, 137, 12, pp. 887-900.

[28] Erdem, S. N., (1988), Tezkiret'ül Bünyan, Binbirdirek Yayınları. İstanbul. (In Turkish)

[29] Frederich, F., (1984), Die Gleislage -aus fahrzeugtechnischer Sicht, Zeitschrift für Eisenbahnwesen und Vekehrstechnik-Glasers Annalen, 108, pp. 355-362. (In German)

[30] Bowles, E. J., (2001), Foundation Analysis and Design. McGraw Hill, London.

[31] Coduto, D. P., (2000), Foundation Design. Prentice Hall, New Jersey.

Cihan Bayındır for the photography and short autobiography, see TWMS J. App. Eng. Math., V.5, N.2.